Lorenzo Miccoli[1], Daniel V. Oliveira[2], Rui A. Silva[2], Anastasios Drougkas[3], Patrick Fontana[1]

[1] Bundesanstalt für Materialforschung und -prüfung (BAM), Berlin, Germany. [2] ISISE University of Minho, Guimarães, Portugal, [3] National Technical University of Athens, Greece

Numerical modelling of rammed earth under different in-plane load conditions

The paper presents a comparison between two different numerical modelling approaches aimed to simulate the in-plain behaviour of rammed earth walls, namely under axial, diagonal and cyclic shear-compression loading. In the first part of the study the mechanical characterisation of wallets tested under uniaxial compression and diagonal compression and walls tested under in-plane cyclic shear-compression loading is presented. The results were used to implement and validate the finite element simulations.

The numerical modelling of the rammed earth samples tested is then discussed in the second part. A non-linear constitutive law based on the total strain rotating crack model (TSRCM) was employed as implemented in the DIANA® software [1]. The aim of the numerical analyses presented here is to simulate the behaviour of rammed earth under different in-plane loading conditions. For the wallets, tests under static loading both macro- and micro-modelling approaches were considered for the simulation of the experimental tests. For the walls subjected to cyclic loading only the micro-modelling approach was applied for the simulation of the experimental tests. The respective FEM model was calibrated with the experimental results. The rammed earth layers were represented by continuum elements, the contact surfaces between layers by interface elements. This approach allowed assessing the influence of the apparent weakness of the interfaces between layers on the shear behaviour of rammed earth.

The goal of the numerical simulation of the cyclic tests was to establish the adequacy of common analytical methods (e.g. used for masonry) applied to the analysis of rammed earth. Rammed earth exhibits brittle characteristics similar to masonry materials and is used in geometrical typologies, such as walls, common in masonry construction.

Experimental programme

Uniaxial compression and diagonal compression tests

A local manufacturer of prefabricated earthen materials (Claytec GmbH, Germany) provided the earth used for the samples. The rammed earth show a bulk density of 2,190 kg/m^3, a particle size range of 0–16 mm and a drying shrinkage of 0.5%. The experimental program consisted in testing five rammed earth wallets under axial compression and another five under diagonal compression. The rammed earth wallets were manufactured with approximate dimensions of 500 × 500 × 110 mm (Fig. 1a). The detailed descriptions of the materials characterisation and static tests are reported elsewhere [2]. The five compression tests were carried out under displacement control, where the testing speed was defined such that the failure occurred within 20-30 min. The axial stress-strain curves obtained from the compression tests of the specimens are presented in Fig. 1b, as well as the respective envelope. These curves thoroughly highlight the non-linear behaviour of rammed under compression, which starts from low stress levels. A typical crack pattern of a rammed earth wallet tested under compression is shown in Fig. 1c. The mechanical properties obtained from compression tests are reported in Table 1.

The five diagonal compression tests were performed following the procedure given in ASTM E 519-10 [3] (Fig. 2a). The tests were carried out under force control at a rate of about 130 N/s up to failure. Fig 2b presents the shear stress–shear strain curves of the specimens, as well as the respective envelope. In general, the wallets exhibited an early peak shear stress, which was followed by shear hardening. It should be noted that the shear hardening phase imparts most of the shear deformations occurring in the tested specimens. A typical crack pattern of a rammed earth

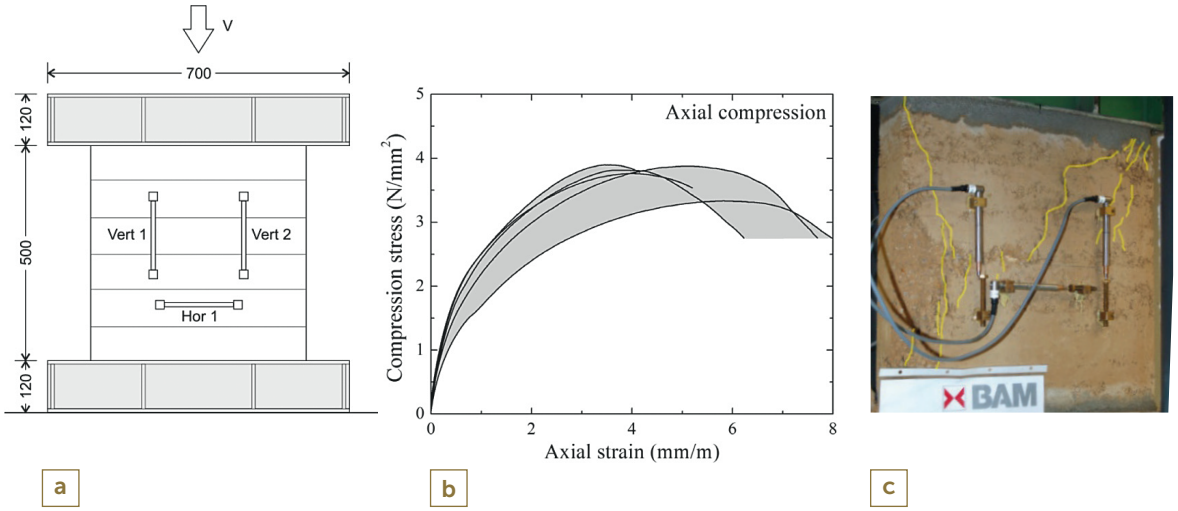

Fig. 1 Compression tests: (a) test setup (dimensions in mm); (b) compression stress–axial strain curves and respective envelope; (c) crack pattern of one of the rammed earth wallet.

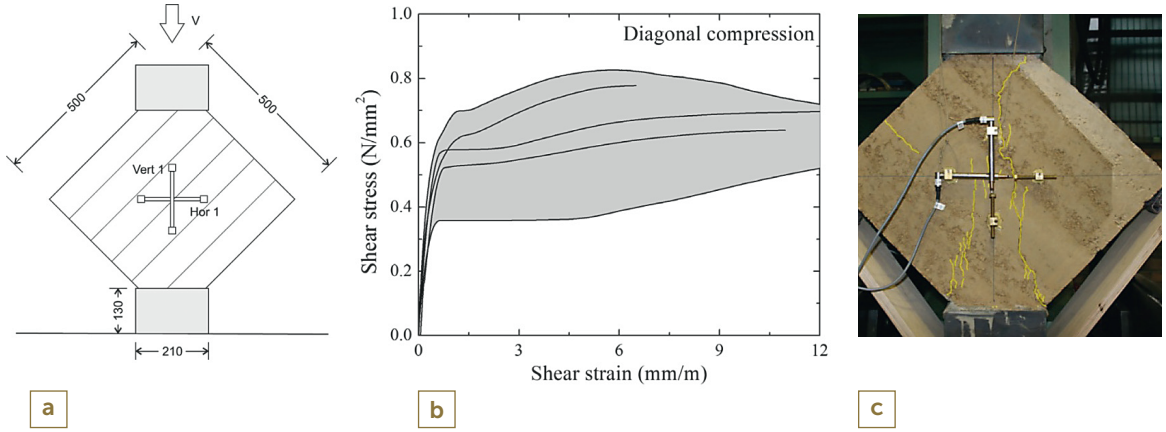

Fig. 2 Diagonal compression tests: (a) test setup (dimensions in mm); (b) shear stress–shear strain curves and respective envelope; (c) crack pattern of one of the rammed earth wallets.

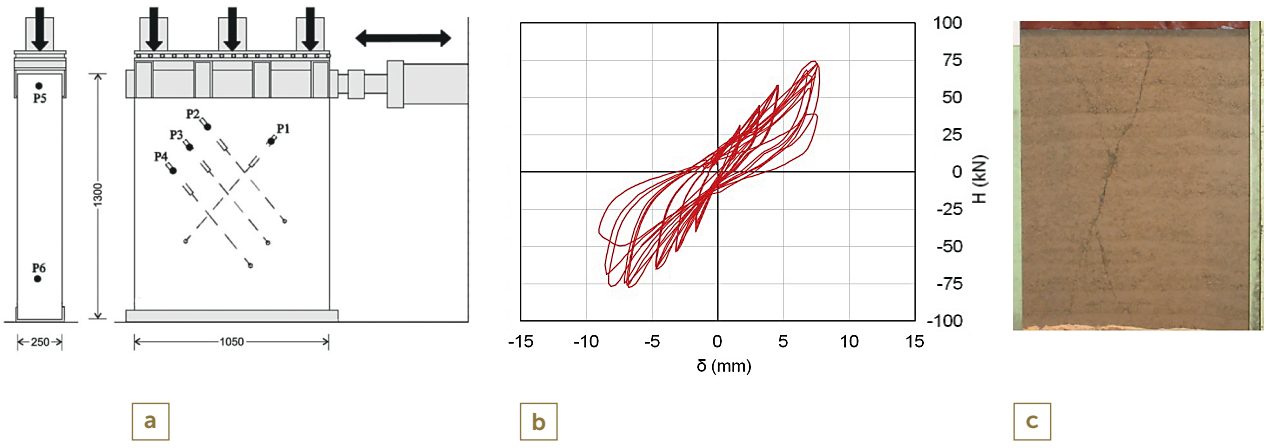

Fig. 3 Cyclic in-plane shear-compression test: (a) scheme of the test and the sensors placement (P1–P6); (b) experimental hysteresis loops; (c) crack pattern of one of the rammed earth walls.

wallet tested under diagonal compression is shown in Fig. 2c. The mechanical properties obtained from the diagonal compression tests are reported in Table 1.

Cyclic shear-compression tests

Three rammed earth walls were manufactured at BAM and used for cyclic shear-compression tests. The walls show a size 1300 × 1050 × 250 mm. The detailed descriptions of samples preparation and cyclic tests are reported elsewhere [4].

Three cyclic in-plane shear-compression tests were carried out at the Institute of Theoretical and Applied Mechanics (ITAM) in Prague. The in-plane cyclic shear-compression tests were carried out following the procedure given in RILEM TC 76-LUMC3 [5]. The test setup with the position of the sensors is shown in Fig. 3a. An imposed vertical compressive stress of 0.56 N/mm^2 was transferred to the wall through three hydraulic jacks by a steel capping beam at the top of the sample.

The hysteresis loops of the horizontal load and the corresponding displacement obtained from the cyclic curves for each step of loading are illustrated in Fig. 3b. The graph shows both the tension and the compression part of the cyclic curves. The typical X-shaped crack pattern along two diagonal lines is shown in Fig. 3c.

All measured load-displacement envelopes show a shape typical for shear failure due to the limited sliding of the rammed earth layers. The maximum values of lateral loads (H), displacements (δ) and corresponding rotation angles (θ) are reported in Table 1.

Numerical Modelling

Initial considerations (geometry, boundary conditions and loading)

Numerical analyses for the simulation of the experimental tests were carried out using a non-linear FEM. A plane stress state was assumed for all models, allowing analysis with lower complexity and computer processing demand. The 2D analysis represents a valid assumption given the geometry of the wallets and the in-plane loading applied. Eight-noded quadrilateral elements (CQ16M) were used to simulate the rammed earth material in both macro- and micro-modelling approaches. In the micro-modelling approach, interfaces between layers were simulated using six-noded zero thickness interface elements (CL12I).

The finite element mesh of the macro-model used to simulate the axial compression tests was constituted by 400 quadrilateral elements. The micro-model was constituted by 480 quadrilateral elements and 100 interface elements, where the thickness of the layers was assumed as 84 mm. The macro-model used to simulate the diagonal compression tests was constituted by 400 quadrilateral elements, while the micro-model was constituted by 460 quadrilateral elements and 100 interface elements.

The boundary conditions adopted in the models simulating the axial compression tests assumed perfect confinement. The load was applied by imposing uniformly distributed vertical displacements on the constrained nodes at the top of the FEM models. The modelling of the diagonal compression tests was carried out in a similar way to that of the axial compression tests.

For the simulation of the cyclic shear-compression tests the numerical model was created using a micro-modelling using continuum and interface elements as for the simulation of the static tests. In addition, two stiff bounding beams were included in the model: one used as foundation and one as top restraint. The base beam was fixed at its foundation and connected to the lowermost rammed earth layer via a non-linear interface. The capping beam was similarly connected to the uppermost rammed earth

Table 1. Results of the static and cyclic tests (standard deviation in brackets)

Uniaxial compression			Diagonal compression		Cyclic shear-compression		
Compressive strength f_c	Young's modulus E_0	Poisson's ratio ν	Shear strength f_s	Shear modulus G_0	Lateral load H_{max}	Displacement δ_{max}	Rotation angle θ_{max}
N/mm^2	N/mm^2		N/mm^2	N/mm^2	kN	mm	%
3.73 (0.23)	4207 (921)	0.27 (0.03)	0.70 (0.11)	1582 (333)	70.37 (9.43)	6.67 (0.51)	0.51 (0.04)

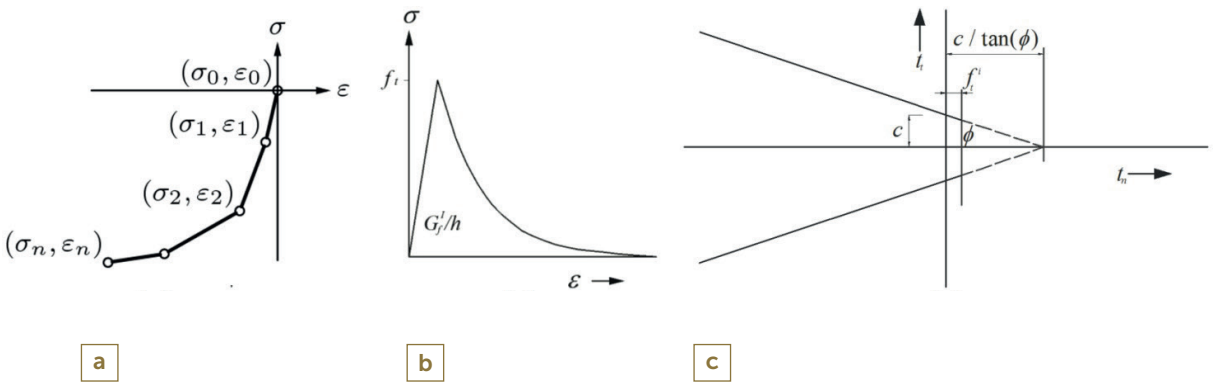

Fig. 4 Material models assumed in the analysis. Stress-strain relationships adopted in the TSRCM: (a) compression (multilinear); (b) tension (exponential); (c) Coulomb friction model used in the modelling of the interfaces between rammed earth layers [1].

layer, but was left free to translate and rotate, as foreseen for the experimental conditions. Overall, 1323 plane stress and 378 interface elements were used in the finite element mesh. A vertical compressive stress was uniformly applied at the top of the capping beam. The cyclic horizontal load was applied as a displacement imposed to the capping beam.

Constitutive laws

A TSRCM was assigned to the continuum elements. This model was able to reproduce the non-linear behaviour of the rammed earth layers in tension and compression. For the compressive behaviour a multilinear curve matching the experimental curves obtained for the materials was assumed (Fig. 4a) and for the tensile behaviour an exponential softening curve (Fig. 4b), both based on fracture energy and finite element crack bandwidth concepts.

The tensile failure criterion was evaluated in the direction of the maximum principal strain and the direction of the crack is fixed upon formation. The crack band width (h) of the elements was assumed to be dependent on the area of the element (A), according to Eq. (1). This assumption allows making the results of the numerical analysis independent from the size of the finite element mesh. This assumption is reasonable for brittle materials, such as rammed earth.

$$h = \sqrt{A}$$

Secant unloading and reloading was assumed, a linear elasticity was assumed for the base and the capping beams. A Mohr-Coulomb frictional failure criterion with a tension cut-off was assigned to the interface elements (Fig. 4c).

This criterion allowed simulating the interfaces' behaviour in combined tension and shear. These interfaces do not represent a physical structural entity, such as a mortar joint. They are able to simulate the mutual interaction of the rammed earth layers as well as, in the case of cyclic loading, between the boundary layers and the two bounding beams.

The values assumed for the parameters are reported in Table 2. The average results obtained from the axial compression tests were used to define the initial values of the compressive strength (f_c), Young's modulus (E_0) and Poisson's ratio (u). The initial values of the remaining parameters were assumed on the base of recommended values for historical masonry. The compressive fracture energy (G_c) was estimated as $1.6f_c$, the tensile strength (f_t) as $0.1f_c$, the mode-I tensile fracture energy (G_f^I) as $0.029f_t$.

For the simulation of the cyclic tests the initial values of the interface normal stiffness (k_n) and of the shear stiffness (k_t) were firstly assumed to be very high, to avoid concentrating the elastic deformations in the interface elements. Therefore, K_n was assumed as $100E_0$ and k_s was estimated using Eq. (2). The cohesion (c) was estimated as a function of the tensile

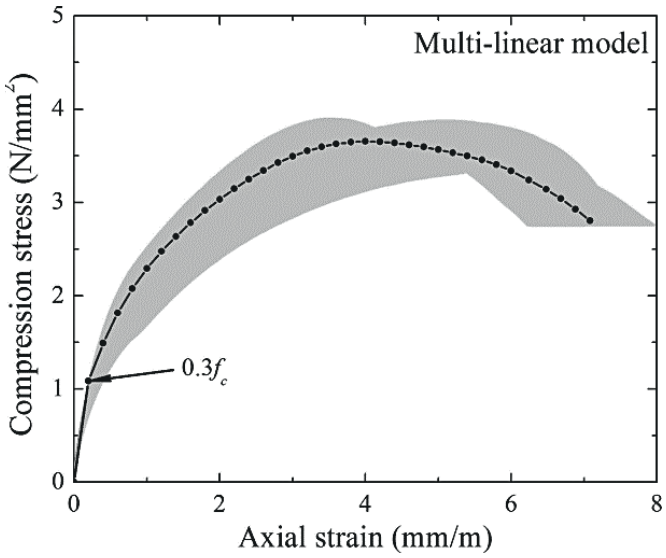

Fig. 5 Multi-linear relationship in compression adopted in the FEM models

strength estimated for the rammed earth, namely as $1.5f_t$. The friction angle (f) was assumed to be 37° and the dilatancy angle (y) as zero. The tensile strength of the interfaces (f_t^i) was defined as $2/3f_t$, while taking into account that the maximum value mathematically allowed by the model is c/tan(f). Finally, the tensile behaviour of the interfaces was assumed as brittle.

$$k_s = \frac{k_n}{2(1+n)}$$

Calibration of the model and results

The calibration of the models consisted in an iterative process where the numerical response was compared against the experimental envelopes. Firstly, the values adopted for the stiffness of the interface elements were assessed by comparing the macro- and micro-model tests. This comparison was carried out by considering the initial values of the parameters, and by increasing and decreasing both in about one order magnitude. Details of this calibration process are reported in previous study [6].

It was decided to use the initial values of the stiffness. A multi-linear relationship was adopted to follow better the pre-peak behaviour in terms of deformability. This relationship was calibrated by taking into account the average curve of the axial compression tests, resulting in the curve depicted in Fig. 5. The second point of the multi-linear relationship was defined for $0.3f_c$ and taking into account the experimental Young's modulus.

Fig. 6a presents the shear stress–shear strain curves of the macro- and micro-model of the diagonal compression tests using the reference values of the parameters and the multi-linear relationship previously calibrated under axial compression. Both models present similar curves and a behaviour much more brittle than that of the experimental curves. This means that the calibration of the models requires adjusting G_f^I, which is the main parameter controlling the brittleness. Fig. 6b depicts the curves of the calibrated models, which resulted from an increase of the initial value of this parameter in about 10 times. This important increase is justified by the fact that rammed earth behaves more as a monolithic material than masonry does.

Fig. 6 Behaviour of the macro- and micro-model of the diagonal compression tests: (a) using the initial parameters; (b) after calibration

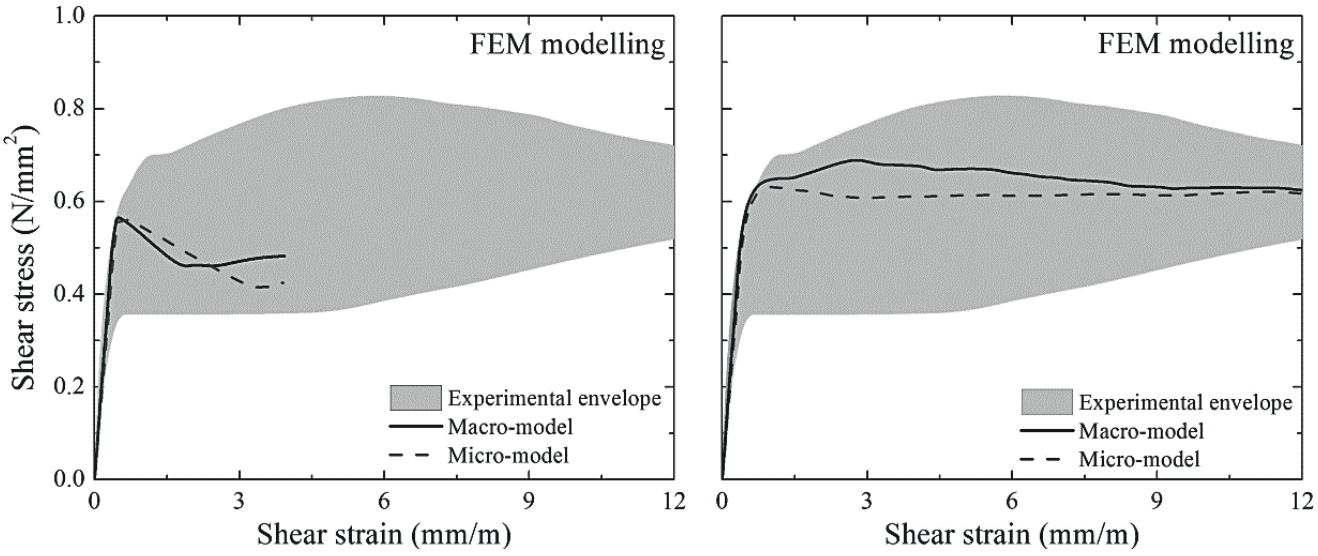

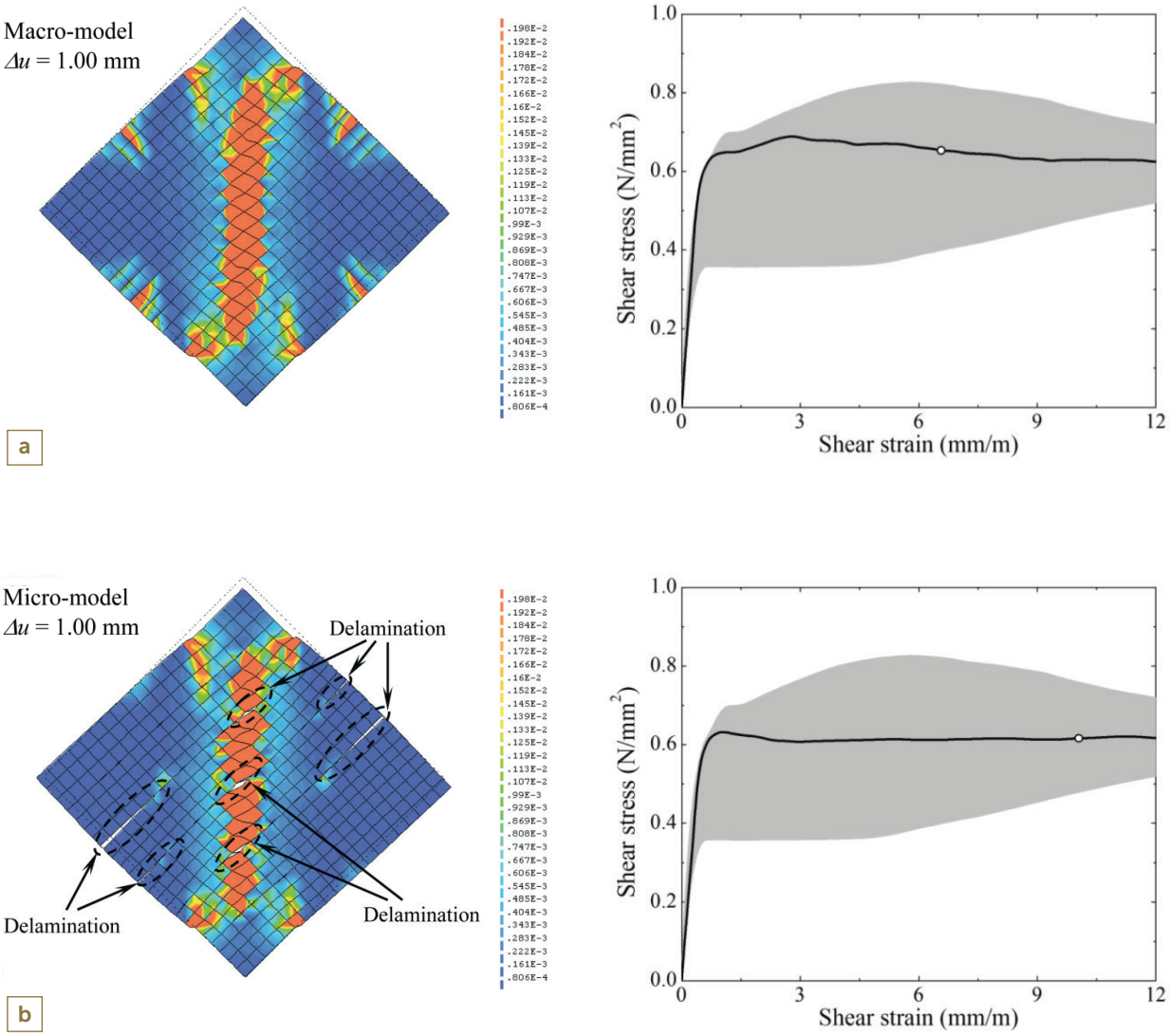

Fig. 7 Principal tensile strains for an imposed vertical displacement (*Du*) of 1 mm: (a) macro-model; (b) micro-model.

The curve of the macro-model is characterized by an early peak shear stress, followed by a small shear hardening until the maximum shear stress is achieved. On the other hand, the curve of the micro-model does not exhibit this early peak shear stress. Instead, the model achieves first the maximum shear stress, followed by a drop in stress with a subtle shear softening. Possibly, this drop in stress is related to the failure of interface elements, which is then compensated with stress redistribution. However, the development of the macro-model curve is closer to those obtained from experimental tests. The macro-model presents higher maximum shear stress than the micro-model, whose values are, respectively, 0.69 N/mm^2 and 0.63 N/mm^2. Both values correspond to a minor underestimation of the average shear strength obtained from the experimental tests (0.70 N/mm^2). In general, it is shown that both curves fit within the experimental envelope, meaning that the use of the TSRCM might provide good results when modelling full rammed earth structures.

The failure modes of both models were also analysed. Fig. 7 presents the tensile principal strains obtained for an imposed vertical displacement of 1.0 mm. The damage of both models is shown to concentrate in the middle, due to the development of tensile stresses, and at the supports, due to stress concentration. This corresponds to the evolution of the system of cracks observed in the experiments.

In the macro-model, damage is also observed to occur at the four borders of the model, which indicates that these regions are vulnerable to the occurrence of delamination failure. The micro-model confirms the occurrence of this failure mode, since it is possible to observe the failure of interface elements at two of the borders, as also observed in the experimental tests. In general, both models are capable of

TSRCM

Material	Young's modulus E_0 N/mm²	Poisson's ratio n	Compressive strength f_c N/mm²	Compressive fracture energy G_c N/mm	Tensile strength f_t N/mm²	Tensile fracture energy G_f^I N/mm
Rammed earth	4207	0.27	3.7	5.98	0.37	0.011

COULOMB FRICTION MODEL

Material	Interface normal stiffness k_n N/mm³	Shear stiffness k_s N/mm³	Cohesion c N/mm²	Friction angle tan(f)	Dilatancy angle tan(y)	Tensile strength of the interface f_t^i N/mm
Interface	4.21×105[a]/42.1[b]	1.66×105[a]/16.6[b]	0.56	0.75	0	0.25

[a] *static loading* [b] *cyclic loading*

Table 2. Values of parameters assumed for numerical modelling

detecting potential zones of failure by delamination. However, the macro-model does not allow controlling this failure mode, neither allows differentiating it from the failure of the rammed earth material.

For the simulation of the walls under cyclic loading, the material properties determined experimentally and fitted through a calibration process were assigned to the rammed earth layers. Since no mechanical characterisation of the layers' interfaces was carried out, nominal values were used for the frictional and tension properties of the interfaces. The elastic properties of the interfaces, namely their elastic stiffness in tension and shear, were determined by means of calibration and matching of the numerical to the experimental results. Ideally, the interfaces ought to be rigid until sliding or opening between the layers occurs. For this reason a high dummy stiffness to the interface was assumed. However, due to imperfections in the compaction process, imperfect contact between layers and disturbance of the interfaces in the actual configuration, this assumption led to a numerical overestimation of the whole wall stiffness. Therefore, the normal stiffness of the interfaces had to be reduced to obtain a wall stiffness comparable to the experimental values. Then the shear stiffness was derived from the normal stiffness according to the equation (2). All the material properties used in the analysis are listed in Table 2.

The results obtained from the numerical analysis are presented in Fig. 8. Dashed curves correspond to the experimental testing, solid curves are related to the numerical simulation. The peak shear force was predicted with a good accuracy, although the whole stiffness of the wall was overestimated in the initial cycles. The accordance between the experimental and the numerical curves is better in the subsequent cycles than in the early ones.

The cracking patterns obtained at the end of the four loading sequences are given in Fig. 9a–d in terms of crack strains, where the orientation of the cracks and the visualisation of the relative crack sizes are shown. The failure mode was dominated by a distinct diagonal cracking, in good agreement with the experimental failure of the layers. Some damages at the interfaces were also registered at the early steps of the analysis.

The micro-model allowed simulating the failure by interface delamination between layers, similar to the one observed in the experimental tests. This result revealed to be the main advantage in utilising the

Fig. 8 Comparison between experimental and numerical hysteresis loops.

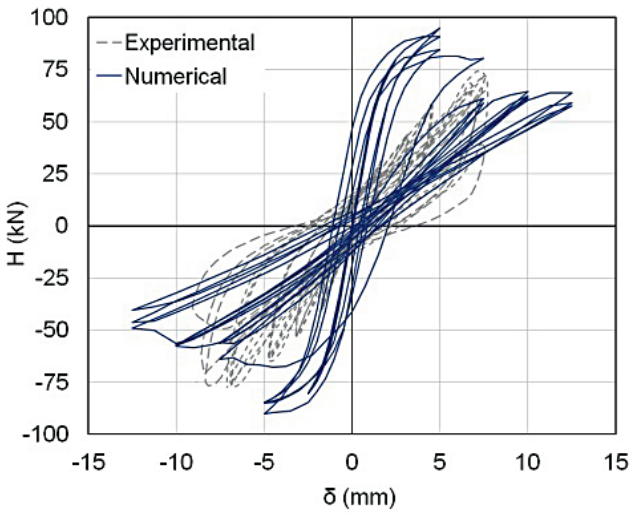

Fig. 9 Evolution of cracking pattern, shown in terms of crack strains, under in-plane cyclic loading at different levels of displacement: (a) 5.0 mm; (b) 7.5 mm; (c) 10.0 mm; (d) 12.5 mm.

micro-modelling approach. This model proved to be sufficiently robust and accurate to simulate the cyclic behaviour of the tested rammed earth walls. However, the approach requires the definition of adequate stress-strain relationships. The micro-modelling approach, where additional computing power is required, is justified when specific collapse mechanisms involving interface failure between layers are expected. In comparison with the simulation of rammed earth under static loading, the interface stiffness as it was used here presented significant differences. The interfaces required elastic stiffness values which were lower than the interfaces used to reproduce the shear behaviour under static diagonal compression.

Conclusions

The non-linear behaviour of rammed earth was modelled by taking into account both the macro- and micro-modelling approaches. The TSRCM was used to simulate the behaviour of the rammed earth material, while the Mohr-Coulomb failure criterion was used to model the interfaces between layers. The experimental results were used in the calibration of the models.

The compression behaviour of the rammed earth was simulated using a multi-linear relationship provided in DIANA software [1]. This relationship was built taking into account the average stress-strain curve of the compression tests. Furthermore, the important non-linear behaviour of rammed earth seems to deem the compression behaviour of this material as non-compatible with relationships traditionally used for modelling concrete. Regarding the simulation of the diagonal compression tests, the calibrated macro- and micro-models demonstrated good comparison with the experimental envelope of the shear stress–shear strain curves and with the experimental damage pattern. The micro-model allowed capturing the failure by delamination of the interfaces between layers, similar to the one observed in the experimental tests. This revealed to be the main advantage of the micro-model approach, yet the macro-model seemed to provide an equivalent numerical simulation of the shear behaviour.

The micro-modelling approach used to model the non-linear behaviour of rammed earth under cyclic loading showed that the calibrated numerical model is in good agreement with the experimental hysteresis loops and their damage pattern. It is worth to underline that the results of the cyclic-shear compression loading are strongly influenced by the significant level of vertical compressive stress employed.

In conclusion, the macro-modelling approach here presented is sufficiently accurate to simulate the global shear behaviour of the rammed earth wallets tested. This approach requires the definition of adequate stress-strain relationships. The use of the micro-modelling approach, where an additional computational effort is required, is justified when specific collapse mechanisms involving failure of the interfaces between layers are expected. It is important to point out the differences of the values of interface stiffness between the static and the cyclic analyses. This difference can be associated with imperfections on the joints in the case of the horizontal loading.

Acknowledgements

This research was funded by the European Commission within the framework of the project NIKER dealing with improving immovable Cultural Heritage assets against the risk of earthquakes (contract No. 244123) and by FEDER funds through the Competitivity Factors Operational Programme – COMPETE, by national funds through FCT – Foundation for Science and Technology within the scope of the projects POCI-01-0145-FEDER-007633 and PTDC/ECM-EST/2777/2014. The authors wish to express their gratitude to Mr André Gardei, and Dr Stanislav Hračov, Dr Stanislav Pospíšil and Mr Shota Urushadze for their important support in the test setup.

References

[1] TNO. Displacement method analyser (DIANA) user's manual. Release 9.4, Netherlands, 2009.

[2] Miccoli L, Müller U, Fontana P. Mechanical behavior of earthen materials: a comparison between earth block masonry, rammed earth and cob. Constr Build Mater 2014;61:327–39.

[3] ASTM E 519-10 (2010) Standard test method for diagonal tension (Shear) in masonry assemblages. American society for testing and materials, West Conshohocken, PA.

[4] Miccoli L, Drougkas A., Müller U, In-plane behaviour of rammed earth under cyclic loading: experimental testing and finite element modelling, Eng Struct 2016; 125, 144-152.

[5] RILEM TC 76. Tests for masonry materials and structures – LUMC3 – Cyclic shear test for masonry panels designed to resist seismic forces; 1991

[6] Miccoli L, Oliveira DV, Silva RA, Müller U, Schueremans L. Static behaviour of rammed earth: experimental testing and finite element modelling. Mater Struct 2015;48:3443–56.